

ARTICLE OPEN



BNT162b2 induces robust cross-variant SARS-CoV-2 immunity in children

Yannic C. Bartsch¹, Jessica W. Chen¹, Jaewon Kang¹, Madeleine D. Burns², Kerri J. St Denis¹, Maegan L. Sheehan¹, Jameson P. Davis², Andrea G. Edlow^{3,4}, Alejandro B. Balazs¹, Lael M. Yonker²✉ and Galit Alter¹✉

Currently available mRNA vaccines are extremely safe and effective to prevent severe SARS-CoV-2 infections. However, the emergence of variants of concerns (VOCs) has highlighted the importance of high population-based vaccine rates to effectively suppress viral transmission and breakthrough infections. While initially left out from vaccine efforts, children have become one of the most affected age groups and are key targets to stop community and household spread. Antibodies are central for vaccine-induced protection and emerging data points to the importance of additional Fc effector functions like opsonophagocytosis or cytotoxicity, particularly in the context of VOCs that escape neutralizing antibodies. Here, we observed delayed induction and reduced magnitude of vaccine-induced antibody titers in children 5–11 years receiving two doses of the age-recommended 10 µg dose of the Pfizer SARS-CoV-2 BNT162b2 vaccine compared to adolescents (12–15 years) or adults receiving the 30 µg dose. Conversely, children mounted equivalent or more robust neutralization and opsonophagocytic functions at peak immunogenicity, pointing to a qualitatively more robust humoral functional response in children. Moreover, broad cross-VOC responses were observed across children, with enhanced IgM and parallel IgG cross-reactivity to VOCs in children compared to adults. Collectively, these data argue that despite the lower magnitude of the BNT162b2-induced antibody response in children, vaccine-induced immunity in children target VOCs broadly and exhibit enhanced functionality that may contribute to the attenuation of disease.

npj Vaccines (2022)7:158; <https://doi.org/10.1038/s41541-022-00575-w>

INTRODUCTION

Rapid vaccine developments and distributions have dramatically mitigated the disease burden of SARS-CoV-2. Children and adolescents, who were mostly spared from the initial surge of COVID-19, were excluded from early vaccine efforts. However, as the pandemic continued, it has become evident that children, too, can suffer from severe COVID-19¹ as well as long-term disease². There has been a marked increase in SARS-CoV-2 cases in children under the age of 18 (<https://services.aap.org/en/pages/2019-novel-coronavirus-covid-19-infections/children-and-covid-19-state-level-data-report/>), potentially fueled by loosened mask mandates³ and the widespread transmission of variants of concern (VOC), including B.1.1.529 (omicron) and its sub-variants⁴. In some areas in the US with low vaccination rates and lack of herd immunity, there is a four-fold increase of hospitalizations in children compared to areas with high vaccine rates⁵. Additionally, children are at risk of developing the severe, post-COVID-19 illness, multi-inflammatory syndrome (MIS-C), weeks after they were exposed to the virus pointing to the importance of vaccine availability to all ages⁶. Moreover, increasing numbers of cases of long-COVID have begun to accrue in children, with unexpected symptoms including brain fog/dizziness, hair loss, stuttering, or palpitations⁷. Meanwhile, mRNA vaccines are available through emergency use authorization (EUA) for children five years and older, however, due to safety and tolerance concerns, mRNA vaccines are available with an adjusted lower dose for children under 12 years of age. It is unclear whether this dose adjustment will negatively impact immunogenicity and lead to a more variable outcome⁸. Moreover, the early unexperienced immune system matures over the first decades of life and

humoral responses to vaccines, including mRNA vaccines can differ considerably to those observed in adults⁹.

Antibodies against SARS-CoV-2 Spike are pivotal correlates of protection from infection and severe COVID-19¹⁰. Currently available mRNA vaccines are able to induce comparably high Spike-specific binding titers across different emerging VOCs¹¹. While antibody-mediated viral neutralization is often used as marker of protection, compared to binding, neutralization is more sensitive to viral evolution in emerging VOCs¹². Along these lines, reduction of in vitro neutralization^{13,14} is not reflected in loss of vaccine protection from severe disease in real-life^{15,16}, and other antibody-mediated effector functions, including opsonophagocytosis, complement activation, and NK cell cytotoxicity, which have less epitope restriction, might be equally important to block transmission and disease^{17,18}. While SARS-CoV-2 vaccines are able to induce broad binding and functional antibodies in adults, whether these responses also emerge in children, particularly in the setting of lower doses in younger children, remains unclear.

Here, to begin to define whether SARS-CoV-2 mRNA vaccines, and particularly the most widely distributed BNT162b2 vaccine, induce functional humoral immune responses in children, we comprehensively profiled vaccine-induced immune responses in 32 children (5–11 years) receiving two doses of BNT162b2 with the age-specific recommended 10 µg dose compared to adolescents (12–15 years, $n = 30$) and adults (16+ years, $n = 9$) receiving the adult 30 µg dose. Despite robust induction of SARS-CoV-2 Spike-specific antibodies, we observed differences in the humoral immune responses across the groups, marked by slower induction and lower antibody titers in the children, but the induction of more robust functionality. While lower in magnitude, VOC-specific

¹Ragon Institute of MGH, MIT, and Harvard, Cambridge, MA 02139, USA. ²Massachusetts General Hospital Department of Pediatrics, Mucosal Immunology and Biology Research Center, Boston, MA 02114, USA. ³Vincent Center for Reproductive Biology, Massachusetts General Hospital, Boston, MA 02114, USA. ⁴Division of Maternal-Fetal Medicine, Department of Obstetrics and Gynecology, Massachusetts General Hospital, Boston, MA 02114, USA. ✉email: LYONKER@mgh.harvard.edu; GALTER@mgh.harvard.edu

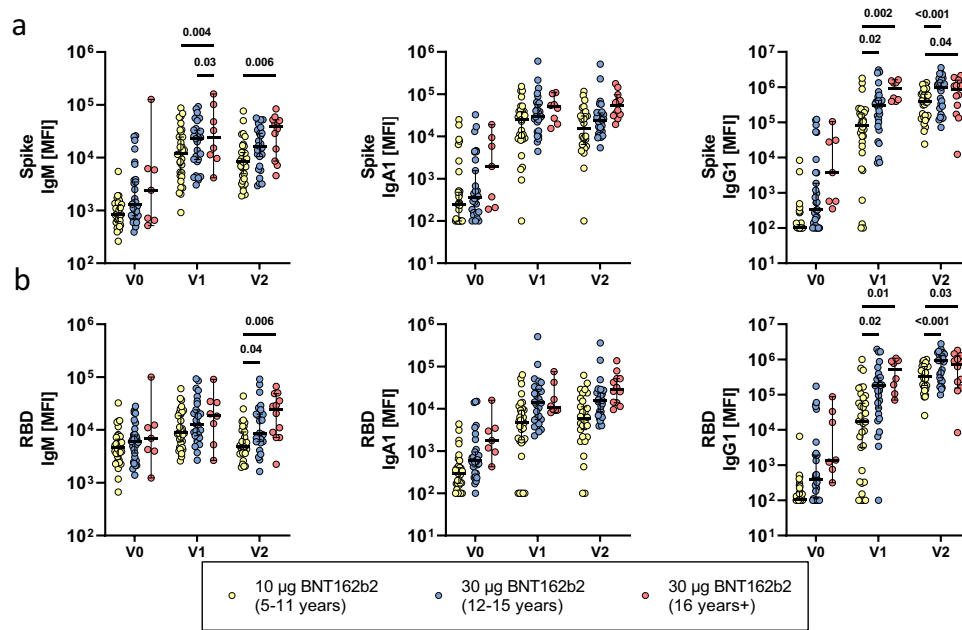


Fig. 1 Vaccination with BNT162b2 mRNA in children results in antibody class switching and produces robust immune response. Relative SARS-CoV-2 wild-type (a) spike (Wuhan) and (b) receptor binding domain (RBD) specific IgM, IgG1, and IgA1 binding levels were determined by Luminex in children receiving either 10 µg of BNT162b2 (ages 5–11 years old, yellow) or 30 µg BNT162b2 (ages 12–16 years old, blue and 16+ years old, red) before (V0_{10µg} (5–11y): 32; V0_{30µg} (12–16y): 29; V0_{30µg} (16+y): 7), after the first dose (V1_{10µg} (5–11y): 32; V1_{30µg} (12–16y): 27; V1_{30µg} (16+y): 8), or after the second dose (V2_{10µg} (5–11y): 30; V2_{30µg} (12–16y): 26; V2_{30µg} (16+y): 11). A two-way ANOVA (two-sided) was used to calculate statistically significant differences between the groups at each timepoint. Exact p-values for statistically significant differences after Benjamini-Hochberg correction for multiple testing are shown above the graph. Horizontal lines indicate the median and error bars the 95% confidence interval.

breadth was comparable across the groups, albeit effector functions to omicron were lowest in the 10 µg dosed children. Collectively, our data point to age and dose-related differences in BNT162b2-induced humoral immunity that may underly differences in the viral breakthrough in the pediatric populations¹⁹ but point to the robust induction of functional humoral immune responses that may confer protection against severe disease across VOCs.

RESULTS

To begin to investigate whether age and dose-dependent differences exist in vaccine-induced antibody profiles across different age groups, we compared the humoral immune response in children 5–11 years old ($n = 32$, median age 9 years, 34% female) receiving the age recommended 10 µg dose to adolescent 12–15 years old ($n = 31$, median age 13 years, 65% female) or adults ($n = 20$, median age 23 years, 60% female) receiving the 30 µg dose BNT162b2. Plasma samples were collected before the first (V0) and second dose (V1) as well as 2–4 weeks after the second dose (V2).

BNT162b2 vaccination elicits robust SARS-CoV-2 specific isotype titers across the different age groups

To compare the humoral immune responses, we analyzed Spike and Receptor binding domain (RBD) specific IgM, IgA and IgG1 isotype titers (Fig. 1). All individuals 12 years and older vaccinated with the 30 µg dose seroconverted (marked by an increase in titer) after the first dose. Likewise, most younger individuals immunized with 10 µg BNT162b2 seroconverted after the first dose (V1). Overall, IgM and IgA Spike and RBD titers tended to be highest in adults, whereas IgG1 titers were higher in the 30 µg vaccinated adolescent group. Furthermore, after one dose, Spike and RBD-specific IgG1 titers were significantly lower in children compared to adolescents ($p = 0.03$) and adults ($p < 0.01$) and titers remained

lower in young children after the second dose. In contrast, epitope-specific responses to the N-terminal domain (NTD) within S1 as well as responses to the S2 domain were more equally recognized across the groups (Supplementary Fig. 1) pointing to a selective deficit in RBD-specific immunity in the youngest group. Interestingly, we noted that some individuals had detectable, albeit low, Spike and RBD-specific IgA and IgG titers at the pre-vaccination (V0) timepoint. None of the participants reported a known previous SARS-CoV-2 infection and serological evidence of pre-exposure, marked by SARS-CoV-2 Nucleocapsid specific IgG1, was not observed (Supplementary Fig. 2). However, these pre-vaccine titers were highly correlated to Spike specific antibodies against the beta-coronavirus OC43 and HKU1, pointing to the existence of cross-coronavirus immunity, as previously reported by other groups^{20–22}. Importantly, the frequency of these responses did not differ across the age groups but they did correlate with the magnitude of the vaccine-induced responses after the 1st or 2nd dose of the vaccine (Supplementary Fig. 3). Collectively, these data argues that BNT162b2 vaccination can induce robust SARS-CoV-2 specific antibody responses in adolescent and adults but result in a more variable response in children 5–11 years old receiving the three-fold lower dose.

Fc effector activity is robust but delayed in children 5–11 years old

Emerging data point to an important role for antibody Fc-effector functions in natural, vaccine-induced, and therapeutic protection against COVID-19^{10,17,18,23–25}. Specifically, in addition to neutralization, antibodies are able to recruit additional effector functions via interactions between their Fc domains and Fc receptors found on all immune cells²⁶. Hence, we analyzed the Fc receptor (FcR) binding properties of SARS-CoV-2 Spike specific antibodies across the three immunized groups (Fig. 2a). After the first dose, more robust cross-FcR-binding profiles were observed in the adolescents and adults, both receiving the 30 µg vaccine dose.

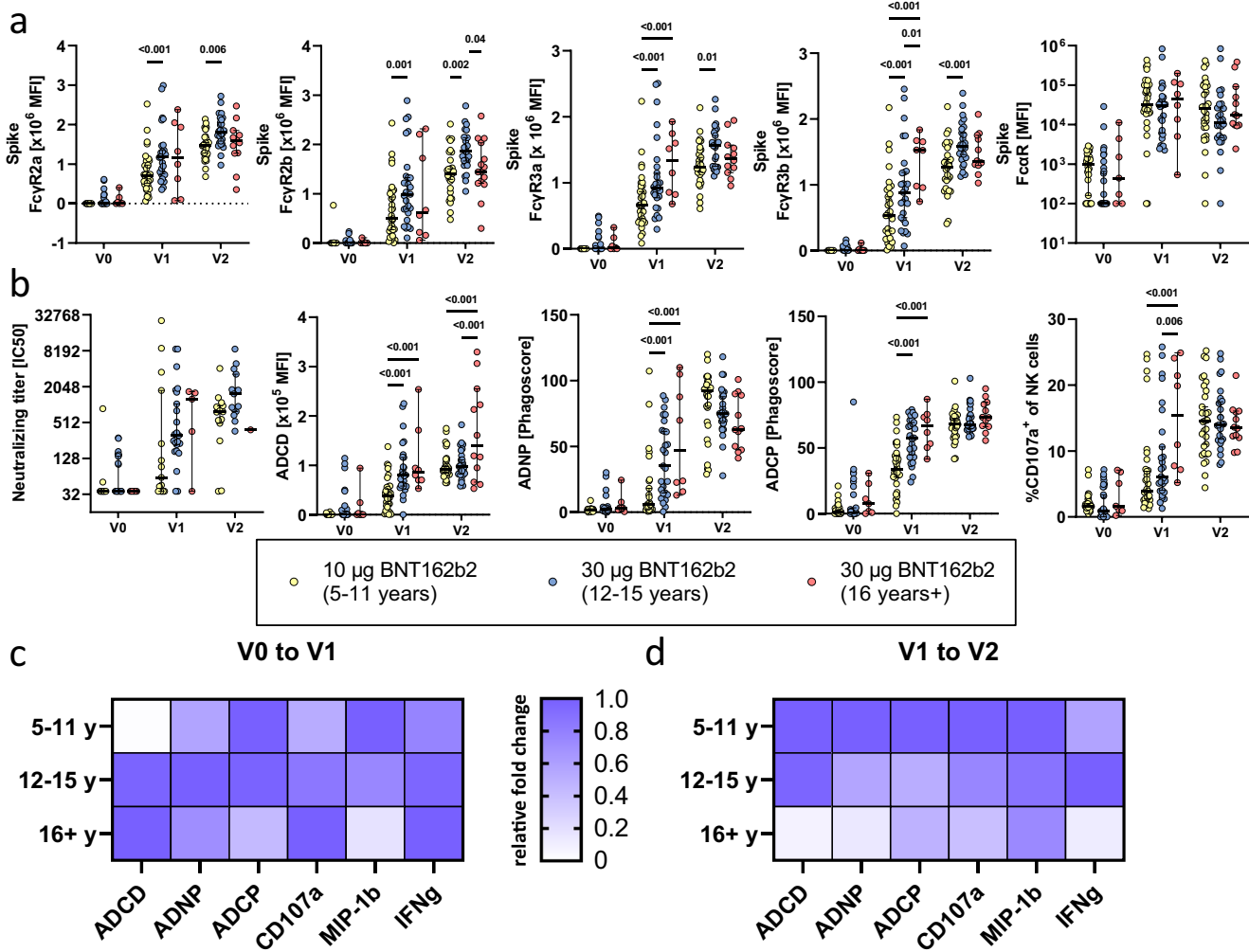


Fig. 2 Vaccination with BNT162b2 mRNA in children induces higher Fc γ R, complement deposition, phagocytic activity, and NK cell activation. **(a)** Binding of SARS-CoV-2 spike specific antibodies to Fc γ R2a, Fc γ R2b, Fc γ R3a, Fc γ R3b and Fc α R determined by Luminex in children receiving 10 μ g of BNT162b2 (ages 5-11 years old, yellow) or 30 μ g BNT162b2 (ages 12-16 years old, blue and 16+ years old, red) before (V0_{10 μ g} (5-11y): 32; V0_{30 μ g} (12-16y): 29, V0_{30 μ g} (16+y): 7), after the first dose (V1_{10 μ g} (5-11y): 32; V1_{30 μ g} (12-16y): 27, V1_{30 μ g} (16+y): 8), or after the second dose (V2_{10 μ g} (5-11y): 30; V2_{30 μ g} (12-16y): 26, V2_{30 μ g} (16+y): 11). **(b)** The ability of SARS-CoV-2 spike specific antibody Fc to induce neutralization, complement deposition (ADCD), neutrophil phagocytosis (ADNP), monocyte phagocytosis (ADCP) and NK cell activation by the frequency degranulated CD107⁺ NK cells. A two-way ANOVA (two-sided) was used to calculate statistically significant differences between the groups at each timepoint. Exact p-values for statistically significant differences after Benjamini-Hochberg correction for multiple testing are shown above the graph. **(c, d)** Heatmaps show the relative fold changes of Fc mediated function before to after the first dose (V0 to V1)(c) or from the first to the second dose (V1 to V2)(d). Horizontal lines indicate the median and error bars the 95% confidence interval.

Interestingly, adults raised Fc γ R3a ($p < 0.001$) and Fc γ R3b ($p \leq 0.03$) responses more rapidly compared to adolescents who received the matching 30 μ g dose. In contrast, after two doses adolescent Fc receptor binding was higher, albeit not significantly, compared to adults across nearly all Fc γ R. Significantly higher binding to the IgG receptors Fc γ R2a ($p_{V1} = 0.001$; $p_{V2} = 0.005$), Fc γ R2b ($p_{V1} = 0.001$; $p_{V2} = 0.002$), Fc γ R3a ($p_{V1} < 0.001$; $p_{V2} = 0.01$) and Fc γ R3b ($p_{V1} = 0.002$ $p_{V2} < 0.001$) was observed in the adolescent group compared the younger 5–11-year-old group after the first and second vaccination. However, 5–11-year-old children mounted similar levels of Fc γ R binding to adults across all Fc γ R, albeit the responses were more variable in young children. Finally, similar binding of IgA to its Fc receptor, Fc α R, were noted across all 3 groups. Thus, adolescents clearly generate more Spike-specific Fc-binding antibodies, with the capacity to bind to FcRs more effectively than adults at the same dose. Conversely, 5-11 years old children induced comparable levels of FcR-binding antibodies, at a lower antibody titer (Fig. 1) compared to adults, suggesting

that children generate qualitatively superior functional antibodies compared to adults.

While antibody titers and FcR-binding levels were more variable in younger children receiving the lower vaccine dose, we next analyzed whether antibody effector profiles differed across the groups (Fig. 2b). While young children clearly required 2 doses of the vaccine to induce robust neutralizing antibody levels, both groups of children raised comparable antibody levels after the 2nd dose, arguing that young children have the capacity to raise nearly equivalent neutralizing antibody titers to adolescents who received a higher dose of the vaccine. Of note, comparable to binding titers, some children and adolescents had pre-existing neutralizing titers potentially related to the presence of cross-reactive antibodies that have been described previously in children^{20–22}. Conversely, more differences were noted across the 3 groups with respect to antibody effector functions. While all Fc effector functions were detected in all groups after the first dose and further enhanced after the second dose (Fig. 2b), the kinetics of evolution of these responses was delayed in the 5-11-

year-old children (Supplementary Fig. 4). Specifically, adolescents and adults generated comparable antibody-dependent complement depositing (ADCD), antibody-dependent neutrophil phagocytic antibodies (ADNP) and antibody-dependent cellular monocyte phagocytosis (ADCP), adults generated superior NK cell activating antibodies (CD107a) after a single dose. Yet, after the second dose, young children who received the low vaccine-dose tended to generate superior ADNP-inducing antibodies and induced comparable ADCP- and ADNKA-inducing antibodies compared to adolescents and adults that received the higher vaccine dose. The relative fold-induction of Fc effector functions after the first dose (V0 to V1) were relatively uniformly enhanced across the groups (Fig. 2c). In contrast, fold-changes after the second dose for all Fc-mediated functions (except IFN γ expression of NK cells which was higher in adolescents) were considerably higher in younger children compared to the adolescent group, and adults exhibited the weakest fold-increase in antibody function after the second dose (Fig. 2d). Given that the magnitude of these functional antibody responses was not significantly different across the groups after the second dose, these data further highlight the importance of the second dose in children, whose antibodies, despite significantly lower subclass/isotype titers, were equally able to induce robust SARS-CoV-2 specific effector functions. Thus, young children experience a unique functional maturation, even at a lower vaccine dose, that may be attributable to their younger, more flexible immune response.

Humoral immune responses are distinct across the groups

Given the various differences in antibody profiles across the age groups, we next aimed to define the specific differences in vaccine responses across age groups that may provide insights on differences in age-dependent immunogenicity profiles. Given that antibody levels, Fc-receptor binding, and function are all highly interrelated, we elected to use a multivariate strategy aimed at rigorously capturing the differences in antibody profiles that explained the greatest level of variance across age-groups. Specifically, focusing on peak immunogenicity, after the complete two dose series, we exploited a Least Absolute Shrinkage and Selection Operator (LASSO) to initially define a minimal set of SARS-CoV-2 specific antibody features that could separate the groups. A minimal set of features was selected to avoid statistical overfitting and define the multivariate features that can explain the variation in antibody profiles across any 2 groups maximally. Using these features, we then used a Partial Least Square Discriminant Analysis (PLS-DA) to visualize the profiles across individual plasma samples (Fig. 3). Thereby, multivariate profiling, unlike univariate profiling, provides insights into the combined vaccine induced features that maximally differ across doses and/or ages. Vaccine-induced antibody Fc-profiles diverged across the children (10 μ g dose) and adolescents (30 μ g dose) (Fig. 3a), marked by elevated levels of Spike-specific IgM, IgA2, IgG1 and IgG3 titers as well as Fc γ R2a binding and IFN γ secretion by NK cells in adolescents. Conversely, vaccine-specific ADNP and NK cell MIP-1 β secretion were selectively enriched in children. Similarly, a comparison of children and adults separated more distinctly in the PLS-DA, with NK cell features, including MIP-1 β and IFN γ production, enriched in children and IgG1, IgA and IgM titers, Fc γ R3b binding, ADCD, and ADCP enriched in adults (Fig. 3b). Interestingly, even adolescent and adult responses differed, despite the matching vaccine dose, marked by age-dependent induction of higher vaccine-specific IgM, IgA and ADCD in adults, but increased binding to Fc γ R2a and monocyte phagocytosis (ADCP) in adolescents (Fig. 3c). These data clearly illustrated that specific differences between children, adolescents and adults exist, where adolescents and adult immune responses were marked by higher antibody titers, but a unique expansion of functional responses was noted in children.

Variable responses to variants of concern after BNT162b2 vaccination

The emergence of variants of concern (VOCs) like the most recent omicron variant has led to continued waves of SARS-CoV-2 infections and breakthroughs globally. Dramatic antigenic changes particularly in the omicron Spike Receptor Binding Domain – important for viral entry – led to near complete loss of vaccine-induced neutralizing antibody titers^{27,28}. However, antibodies are still able to sense other parts of Spike VOCs, elicit Fc effector functions, and thereby potentially mediate protection from severe disease. However, whether vaccination in children leads to recognition of VOCs is unclear. Thus, we next analyzed the specific humoral response to different VOCs, including alpha (B.1.1.7), beta (B.1.351), gamma (P.1), delta (B.1.617.2) and omicron (B.1.1.529) at peak immunogenicity (Fig. 4). Despite the lower antibody titers in children, all 3 groups exhibited more stable IgA and IgG binding across the alpha, beta, gamma, and delta VOCs, but compromised recognition of omicron (Fig. 4a and Supplementary Fig. 5). IgM binding antibodies were significantly impaired in recognition of the omicron Spike, but exhibited enhanced recognition of other VOCs, pointing to an isotype-specific compromised response to this more mutated VOC, however, all 3 groups clearly adapted their more mature IgA and IgG responses to compensate for this deficit in IgM immunity. Unexpectedly, IgM reactivity to the Beta variant was improved in children and adolescents compared to the D614G response pointing to age-dependent differences in the evolution of breadth of binding across VOCs. Moreover, fold changes of binding over D614G across isotype and FcR-binding titers to different VOC full Spike and RBDs highlighted consistent patterns of breadth of binding across VOCs across the age groups (Fig. 4b), with the exception of IgM binding in children and adolescents that was superior across all VOCs, except omicron. These data point to a unique flexibility in cross-reactivity in IgM in children. Given the robust opsonophagocytic and complement-fixing function of IgM, these data point to a unique capability programmed in children that may help provide some level of persistent broad recognition of VOCs following vaccination.

While antibody binding to most VOC Spikes was largely preserved, there was an apparent reduction for the omicron variant recognition across all ages. We therefore profiled the ability of vaccine-induced antibodies to elicit neutralizing and Fc-mediated effector functions to omicron (Fig. 4c and Supplementary Fig. 5). As expected, omicron-specific antibody effector functions were detectable but reduced when compared to D614G Spike-specific responses after first and second dose of BNT162b2. Children receiving the 10 μ g dose, showed lower omicron-specific reactivity at both timepoints compared to adult-dosed adolescent or adults. Interestingly, while the omicron-specific effector profiles expanded from the first to the second dose in the 10 μ g dosed children and 30 μ g dosed adolescents, ADNKA and ADCP to omicron were reduced from the first to the second dose in adults. Collectively, our data indicate that while adults produce sufficient effector responses after the first vaccine dose, adult immunity becomes narrower towards the vaccine insert antigen after the second dose. In contrast, children and adolescents may not be fully primed after the first dose but develop a broad and highly functional vaccine response after the full vaccine series.

DISCUSSION

Early in the pandemic, pediatric cases accounted for approximately 5% of the total COVID-19 cases in the US. Reasonably, initial vaccine campaigns focused on the protection of adults. Since then, pediatric cases of SARS-CoV-2 have exceeded 13 million with over 42,000 hospitalizations, resulting in the

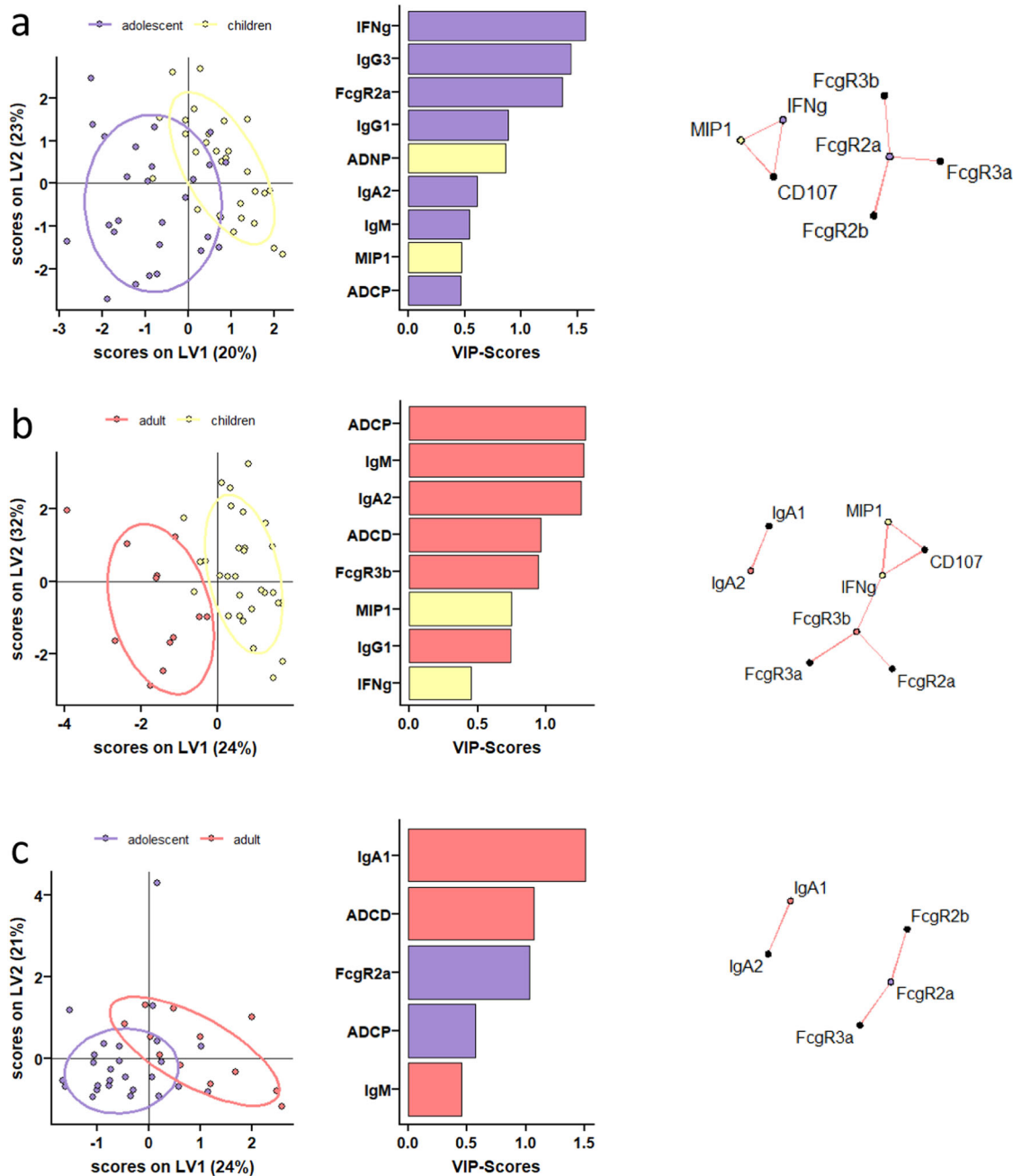


Fig. 3 Distinct humoral profiles between BNT162b2 mRNA vaccinated pediatric children, adolescent children, and adults against SARS-CoV-2 wild-type spike. (a-c) A machine learning model was built using LASSO selected SARS-CoV-2 wild-type spike specific features at V2. Vaccine response in adolescent children (purple) and pediatric children (yellow) given 10 μ g BNT162b2 (a), in adults (red) and pediatric children (yellow) given 30 μ g BNT162b2 (b), or in adults (red) and adolescent children (purple) given 30 μ g BNT162b2 (c) were compared. Separation of the groups in the PLS-DA is shown in the right panel. Variable importance (VIP) score of LASSO selected features is shown in the bar graph and features are color coded by the group they were enriched in. The network plots (right panel) show significant ($p < 0.05$) Spearman correlations ($|r| > 0.7$, only positive correlations were observed) to other (non-selected) features.

emergency use authorization for mRNA vaccines for children 5 years of age and older. However, due to the delayed vaccine rollout and increased vaccine hesitancy by parents, vaccination rates in children still lag behind. Together with the occurrence of emerging variants like omicron accompanied by relaxed masking and social distance measurements, cases of COVID-19 have soared with up to 20% of the total SARS-CoV-2 infections occurring in children during the recent omicron wave. In addition to acute infection, children are at special risk of developing a severe multi-inflammatory syndrome (MIS-C) weeks after asymptomatic SARS-

CoV-2 exposure. Importantly, data indicates that 30 μ g BNT162b2 not only protects adolescents (12–18 years) from severe COVID-19 but also MIS-C²⁹, underscoring the importance and effectiveness of vaccination across the ages.

As innate and adaptive immune systems mature during the first decades of life, it was not clear how the naïve, pediatric immune system would respond to mRNA vaccine technology. Furthermore, due to safety and tolerance concerns, doses were adjusted for the younger 5–11-year-old age group. Our data point to a more variable immune response in children 5–11 years of age receiving

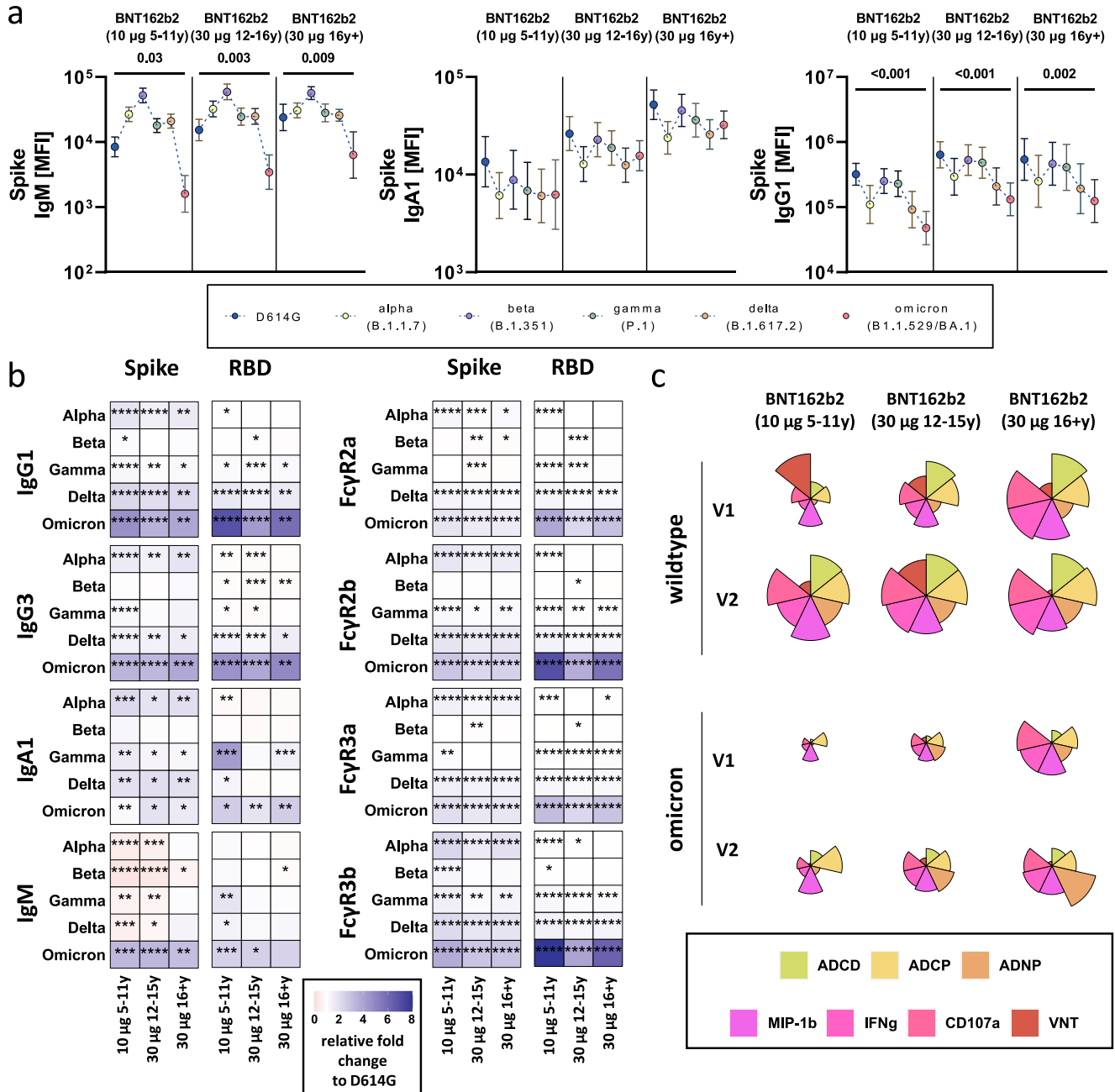


Fig. 4 SARS-CoV-2 variants of concern specific humoral immune responses after vaccination with BNT162b2. (a) Vaccine-induced IgM, IgA1, and IgG1 response to D614G (wild-type; blue), alpha (B.1.1.7, yellow), beta (B.1.1.7, purple), gamma (P.1, green), delta (B.1.617.2, orange), and omicron (B.1.1.529/BA.1, red) to the full Spike in children receiving 10 µg of BNT162b2 (ages 5-11 years old, $n = 30$) or adolescents receiving 30 µg BNT162b2 (ages 12-15 years old, $n=26$) or adults (16 + years old, $n=17$) at V2. Geometric mean of each group is shown, error bars indicate the 95% confidence interval (CI). A two-sided Kruskal-Wallis test with Benjamini-Hochberg correction for multiple testing was performed to compare D614G and omicron-specific antibody titers. P-values for significant different comparisons are shown above the dataset. (b) Heatmaps show the relative fold change (red = increase, white = no change, blue = decrease) for the different VOCs compared to the original D614G variant for Spike and RBD-specific IgG1, Ig3, IgA1 and IgM titers or binding to FcγR2a, FcγR2b, FcγR3a, FcγR3b. (c) Flower plots summarize AD/CD, AD/CP, AD/NP, AD/NKA (CD107a, IFNγ, MIP-1β) and neutralization (VNT) at V1 and V2 against D614G (upper panel) or omicron (lower panel) Spike in 10 µg of BNT162b2 (ages 5-11 years old) or adolescent receiving 30 µg BNT162b2 (ages 12-15 years old) or adults (16 + years old) at V2. Each petal represents a specific function (compare color key) and the length of the petal corresponds of the intensity of Z-scored and normalized data. Asterisks in (b) indicate significant differences of the respective variant in a paired two-sided Wilcoxon rank test. P-values were corrected for multiple testing using Benjamini-Hochberg correction. $*:p < 0.05$, $** :p < 0.01$, $***:p < 0.001$, $****:p < 0.0001$.

a three-fold lower dose BNT162b2 compared to adolescents and adults. Analysis of a dose-down study of the Moderna mRNA-1273 vaccine suggests that children have an attenuated immune response after a two-fold lower dose, though, age-specific differences may have also accounted for this²⁵. Here, we noted

a selective humoral deficiency in isotype and Fc receptor binding titers after one dose of BNT162b2 in children and adolescents compared to adults. Yet, humoral immunity expanded robustly after the second dose, raising functions to levels comparable or superior to those observed in adults, with titers in the adolescent

group exceeding those in adults. Moreover, after two doses, children had specifically elevated highest levels of opsonophagocytic and NK cell activating antibodies that have been previously associated with resolution of severe disease^{30,31}. This enhanced functionality could be attributable to a variation in epitope selection or post-translational modification of the antibody Fc-domain that collectively could alter the quality of the pediatric immune response antibody quality. For example, emerging data point to striking differences in antibody Fc-glycosylation across the ages resulting in the generation of more pro-inflammatory antibodies in the earliest years of life, which are associated with increased NK cell activation in COVID-19^{32,33}. While we were limited by the amount of available pediatric samples for antibody glycosylation analysis, future studies may provide enhanced insights on the specific vaccine-induced antibody changes that may permit children to generate more functional antibodies at a half-vaccine dose compared to adolescents or adults. Furthermore, antibody avidity was higher in adolescents and adults (Supplementary Fig. 3) pointing to qualitative differences in the response to mRNA vaccination in children, adolescents and adults. Additionally, whether a matched adult dose of mRNA or expanded interval between vaccine doses could further expand and improve the 5-11-year-old immune response remains unclear but warrants further investigation into dose-dependent immune programming across the ages to guide future mRNA vaccine design. Furthermore, while the cohort was small, we noted slight influences of sex on vaccine-induced antibody profiles (Supplementary Fig. 6) largely at the time of puberty. Thus, future studies with larger numbers of children, across the ages, across puberty, and powered to probe additional co-variants, including body weight, ethnicity or pre-existing co-morbidities, may provide further insights into the host-factors that may modulate immunogenicity and ultimately shape population-level vaccine efficacy.

Since the beginning of the SARS-CoV-2 pandemic, cross-reactive antibodies, and repetitive exposure of young individuals to other circulating coronaviruses have been discussed as potential contributors to shaping SARS-CoV2 immunity and providing protection against severe disease²⁰. While causal evidence is still missing, several studies have described the existence of pre-pandemic cross-reactive antibodies or T cell epitopes to SARS-CoV-2 that have appear to reduce disease severity^{34,35}. Moreover, other studies have argued that the sequence of VOC exposure can lead to original antigenic sin restricting the quality and breadth of the overall humoral immune response^{36,37}. Interestingly, vaccine-induced IgA was able to effectively recognize VOC Spike, and thus, might directly contribute to recognition of different VOCs at mucosal surfaces. Likewise, we noted pre-existing SARS-CoV-2 Spike-specific antibodies able to mediate neutralization and elicit Fc effector functions, in the absence of evidence of previous infection (Supplementary Fig. 2). Along these lines, immune responses to common coronaviruses, such as the Beta-coronaviruses HKU1 and OC43, were correlated to antibody binding to SARS-CoV-2 Spike across populations (Supplementary Fig. 3). Furthermore, BNT162b2 vaccination boosted pre-existing and elicited OC43 specific antibodies and was associated with post-vaccine titers across the groups, pointing to limited evidence of original antigenic sin. Moreover, children induced robust cross-VOC IgG and IgA responses, and even enhanced IgM responses, to all VOCs tested other than omicron. Thus, these data suggest that pre-existing immunity is unlikely to limit the development of antibodies to more related SARS-CoV-2 VOCs (e.g., after natural infection or VOC-specific vaccination). Yet, strategies to augment breadth to more disparate spike variants, such as omicron, are urgently needed for both children and adults. Additionally, other immune mechanisms, including T cells may also continue to recognize and protect from infections. Thus, it will be critical to characterize T cell responses and humoral stability of the more variable response in young children to guide booster

immunization guidelines and to shape future mRNA vaccine strategies in children.

METHODS

Sample collection

Participants were invited to participate in this study and donate blood samples prior to the first regular vaccination. Pediatric samples were collected from children vaccinated with either 10 µg BNT162b2 ($n = 32$, ages 5–11 years old) or 30 µg BNT162b2 (ages 12+ years old, $n = 31$) or 16 years and older ($n = 20$) as a part of FDA's emergency use authorization of the BNT162b2 vaccine for these age groups (November 2021 and May 2021, respectively). Sera were collected prior to vaccination (V0), before the second dose approximately 3 weeks after the first dose of Pfizer-BioNTech mRNA vaccination (V1), and/or two to four weeks after the second dose (V2). All individuals over 18 years of age, or parents/legal guardians of children under age 18 years gave informed consent prior to enrollment. All children provided assent. Written consent and assent was obtained, except when limitations arose related to the COVID-19 pandemic, in which case verbal consent and assent was obtained and recorded. All study procedures were approved by the MassGeneralBrigham Institutional Review Board (#2020P000955 or #2021P002628).

Cell lines and primary cells

THP-1 cells, a human leukemia monocyte cell line, were maintained in RPMI-1640 Medium (Sigma-Aldrich) with 10% fetal bovine serum (FBS, Sigma-Aldrich), 1% L-glutamine (Corning), 2% of 5000 IU/mL of Penicillin and 5,000 µg/ml of Streptomycin Solution (Pen-Strep, Corning), 1% of 1 M HEPES (Corning), and 5 mM 2-Mercaptoethanol (Gibco). Cells were incubated at 37 °C with 5% CO₂.

Primary neutrophils for antibody-dependent neutrophil phagocytosis (ADNP) assays were isolated from whole blood from healthy donors using Ammonium-Chloride-Potassium (ACK) Lysing Buffer (Quality Biological) followed by centrifugation and multiple wash steps prior to assay usage.

Primary natural killer cells for the antibody-dependent natural killer activation (ADNKA) assays were isolated from buffy coats from healthy donors using the RosetteSep NK cell enrichment kit (STEMCELL Technologies). Cells were incubated overnight at 37 °C with 5% CO₂ in RPMI-1640 Medium (Sigma-Aldrich) with 10% FBS (Sigma-Aldrich), 1% L-glutamine (Corning), 2% of Pen-Strep (Corning), and 1% of 1 M HEPES (Corning) prior to assay usage.

Human embryonic kidney (HEK) 293 T cells expressing ACE2 for neutralization assays were maintained in Dulbecco's Modified Eagle's Medium (DMEM, Corning) with 10% FBS (VWR) and 1% Pen-Strep (Corning) and incubated in 37 °C with 5% CO₂.

Antigens and biotinylation

Antigens were biotinylated using the NHS-Sulfo-LC-LC kit following manufacturer's instructions (ThermoFisher). Excess biotin was removed via size exclusion chromatography by using Zeba-Spin desalting columns (7 kDa cutoff, ThermoFisher).

Antibody isotype and Fc receptor binding

Antigen-specific antibody isotype, subclass, and Fc receptor binding profiles were analyzed using a custom multiplex Luminex assay³⁸. The antigens were coupled directly onto the Luminex microspheres (Luminex Corp) via carboxy coupling. Coupled beads were incubated with diluted plasma samples overnight at 4 °C. Following overnight incubation, non-specific antibodies were washed off and the immune complexes were incubated with Ig isotypes or subclasses with a 1:100 diluted PE-conjugated secondary antibody for IgG1 (clone: HP6001), IgG2 (clone: 31-7-

4), IgG3 (clone: HP6050), IgG4 (clone: HP6025), IgM (clone: SA-DA4), IgA1 (clone: B3506B4), or IgA2 (clone: A9604D2) (all Southern Biotech). For avidity analysis, immune-complexes were incubated for 10 min with 2.5 M urea or PBS (no urea control) prior to PBS wash and addition of the IgG1 secondary probe. For the FcγR binding, the secondary probe is a PE-streptavidin (Agilent Technologies) coupled recombinant and biotinylated human FcγR protein. Beads with secondary antibodies were incubated on a shaker at room temperature for 1 hour. Following incubation, excessive antibodies were washed off and relative antigen-specific antibody levels were determined on an iQue analyzer (Intellicyt).

Antibody-dependent complement deposition (ADCD) assays

For the ADCD assays³⁹, biotinylated antigens were coupled to FluoSphere NeutrAvidin beads (ThermoFisher). Immune complexes were formed by incubating antigen coupled beads with 10 ul of 1:10 diluted plasma samples at 37 °C for 2 hours. Following incubation, non-specific antibodies were washed off followed by incubation of the immune complex with guinea pig complement in GVB ++ buffer (Boston BioProducts) at 37 °C for 20 min. To stop the complement reaction, 15 mM EDTA (Corning) in PBS was added to the immune complex. C3 deposited on beads were stained with anti-guinea pig C3-FITC antibody (MP Biomedicals, 1:100, polyclonal) and analyzed on an iQue analyzer (Intellicyt).

Antibody-dependent neutrophil phagocytosis (ADNP) assays

For the ADNP assays⁴⁰, biotinylated antigens were coupled to FluoSphere NeutrAvidin beads (ThermoFisher). Immune complexes were formed by incubating antigen coupled beads with 10 ul of 1:50 diluted plasma samples at 37 °C for 2 hours. Primary neutrophils were isolated as previously mentioned and 50,000 cells per well incubated with washed immune complexes at 37 °C for 1 hour. Following incubation, neutrophils were stained for surface CD66b (Biolegend, 1:100, clone: G10F5) expression and fixed with 4% para-formaldehyde. Analysis was done on an iQue analyzer (Intellicyt).

Antibody-dependent cell phagocytosis (ADCP) assays

For the ADCP assays^{41,42}, biotinylated antigens were coupled to FluoSphere NeutrAvidin beads (ThermoFisher). Immune complexes were formed by incubating 10 ul of antigen coupled beads with 10 ul of 1:100 diluted plasma samples at 37 °C for 2 hours. THP-1 monocytes (25,000 cells per well) were then added to the beads then incubation at 37 °C for 16 hours. Following incubation, cells were fixed with 4% para-formaldehyde and analyzed on an iQue analyzer (Intellicyt).

Antibody-dependent NK activation (ADNKA) assays

MaxiSorp ELISA plates (ThermoFisher) were coated with either 1 μg/ml SARS-CoV-2 wt spike or omicron variant spike at room temperature for 2 hours followed by blocking with 5% BSA (Sigma-Aldrich). 50 ul of 1:50 diluted plasma samples were added to the wells and incubated overnight at 4 °C. Primary NK cells were prepared as described above. Cells were added to the washed ELISA plate and incubated with anti-human CD107a (BD, 1:40, clone: H4A3), brefeldin A (Sigma-Aldrich) and monensin (BD) at 37 °C for 5 hours. Following incubation, cells were surface stained for CD56 (BD, 1:200, clone: NCAM16.2) and CD3 (BD, 1:200, clone: UCHT1). The NK cells were then washed, fixed, and permeabilized using the Fix & Perm Cell Permeabilization Kit (ThermoFisher). Cells were then stained for intracellular markers MIP1β (BD, 1:50, clone: D21-1351) and IFNγ (BD, 1:17, clone: B27). NK cell populations were defined to be CD3-CD56 +. The frequency of degranulated cells marked by CD107a and the expression of intracellular IFNγ and MIP-1β were determined on an iQue analyzer (Intellicyt).

Virus neutralization

Three-fold serial dilutions of plasma samples starting at 1:12 or 1:30 were performed before adding pseudovirus expressing either SARS-CoV-2 wild-type spike or omicron variant spike to HEK293T expressing ACE-2 cells for 1 hour. Pseudoviruses were produced by PEI transfection of lentiviral vector with CMV-Luciferase-IRES-ZsGreen, lentiviral helper plasmids, and either SARS-CoV-2 wt spike or omicron variant spike expression plasmid. Pseudovirus neutralization titers (pNT50) values were calculated by taking the inverse of 50% inhibitory concentration value for all samples with a pseudovirus neutralization value of 80% or higher at the highest concentration of serum.

Data analysis and statistics

Data analysis was performed on GraphPad Prism (v.9.3) and RStudio (v.1.3). A two-way ANOVA test with Benjamini-Hochberg correction for multiple testing in GraphPad Prism was used to determine statistically significant differences between the groups at each timepoint. Flower plots were generated with the ggplot package in R using Z-scored data. Multivariate classification models were built to discriminate between humoral profiles of vaccination arms. Feature selection was performed using the least absolute shrinkage and selection operator (LASSO) and classification and visualization were performed using partial least square discriminant analysis (PLS-DA). These analyses were performed using R package “ropls” version 1.20.0⁴³ and “glmnet” version 4.0.2⁴⁴. Co-correlate networks were built using Spearman method followed by Benjamini-Hochberg correction and the co-correlate network was generated using R package “network” version 1.16.0⁴⁵.

Reporting summary

Further information on research design is available in the Nature Research Reporting Summary linked to this article.

DATA AVAILABILITY

All relevant data are included in this manuscript. No data was stored externally.

CODE AVAILABILITY

No custom code was used in this study.

Received: 6 June 2022; Accepted: 3 November 2022;

Published online: 03 December 2022

REFERENCES

- Swann, O. V. et al. Clinical characteristics of children and young people admitted to hospital with covid-19 in United Kingdom: prospective multicentre observational cohort study. *BMJ* **370**, m3249 (2020).
- Stephenson, T. et al. Long COVID and the mental and physical health of children and young people: national matched cohort study protocol (the CLoCK study). *BMJ Open* **11**, e052838 (2021).
- Donovan, C. V. et al. SARS-CoV-2 Incidence in K-12 School Districts with Mask-Required Versus Mask-Optional Policies - Arkansas, August-October 2021. *MMWR Morb. Mortal. Wkly Rep.* **71**, 384–389 (2022).
- Marks, K. J. et al. Hospitalizations of Children and Adolescents with Laboratory-Confirmed COVID-19 - COVID-NET, 14 States, July 2021-January 2022. *MMWR Morb. Mortal. Wkly Rep.* **71**, 271–278 (2022).
- Siegel, D. A. et al. Trends in COVID-19 Cases, Emergency Department Visits, and Hospital Admissions Among Children and Adolescents Aged 0-17 Years - United States, August 2020-August 2021. *MMWR Morb. Mortal. Wkly Rep.* **70**, 1249–1254 (2021).
- Feldstein, L. R. et al. Multisystem Inflammatory Syndrome in U.S. Children and Adolescents. *N. Engl. J. Med.* **383**, 334–346 (2020).
- Zimmermann, P., Pittet, L. F. & Curtis, N. How Common is Long COVID in Children and Adolescents. *Pediatr. Infect. Dis. J.* **40**, e482–e487 (2021).

8. Press Release Pfizer Inc and BioNTech SE PFIZER AND BIONTECH PROVIDE UPDATE ON ONGOING STUDIES OF COVID-19 VACCINE. (2021).
9. Bonhoeffer, J., Siegrist, C. A. & Heath, P. T. Immunisation of premature infants. *Arch. Dis. Child* **91**, 929–935 (2006).
10. Gilbert, P. B. et al. Immune correlates analysis of the mRNA-1273 COVID-19 vaccine efficacy clinical trial. *Science* **375**, 43–50 (2022).
11. Kaplonek, P. et al. mRNA-1273 and BNT162b2 COVID-19 vaccines elicit antibodies with differences in Fc-mediated effector functions. *Sci. Transl. Med* **14**, eabm2311 (2022).
12. Pegu, A. et al. Durability of mRNA-1273 vaccine-induced antibodies against SARS-CoV-2 variants. *Science*, <https://doi.org/10.1126/science.abj4176> (2021).
13. Wu, K. et al. Serum Neutralizing Activity Elicited by mRNA-1273 Vaccine. *N. Engl. J. Med* **384**, 1468–1470 (2021).
14. Liu, Y. et al. Neutralizing Activity of BNT162b2-Elicited Serum. *N. Engl. J. Med* **384**, 1466–1468 (2021).
15. Abu-Raddad, L. J., Chemaitelly, H. & Butt, A. A., National Study Group for, C.-V. Effectiveness of the BNT162b2 Covid-19 Vaccine against the B.1.1.7 and B.1.351 Variants. *N. Engl. J. Med* **385**, 187–189 (2021).
16. Charmet, T. et al. Impact of original, B.1.1.7, and B.1.351/P.1 SARS-CoV-2 lineages on vaccine effectiveness of two doses of COVID-19 mRNA vaccines: Results from a nationwide case-control study in France. *Lancet Reg. Health Eur.* **8**, 100171 (2021).
17. Gorman, M. J. et al. Fab and Fc contribute to maximal protection against SARS-CoV-2 following NVX-CoV2373 subunit vaccine with Matrix-M vaccination. *Cell Rep Med*, 100405, <https://doi.org/10.1016/j.xcrm.2021.100405> (2021).
18. Atyeo, C. et al. Distinct Early Serological Signatures Track with SARS-CoV-2 Survival. *Immunity* **53**, 524–532 e524 (2020).
19. Fowlkes, A. L. et al. Effectiveness of 2-Dose BNT162b2 (Pfizer BioNTech) mRNA Vaccine in Preventing SARS-CoV-2 Infection Among Children Aged 5–11 Years and Adolescents Aged 12–15 Years - PROTECT Cohort, July 2021–February 2022. *MMWR Morb. Mortal. Wkly Rep.* **71**, 422–428 (2022).
20. Ng, K. W. et al. Preexisting and de novo humoral immunity to SARS-CoV-2 in humans. *Science* **370**, 1339–1343 (2020).
21. Wratil, P. R. et al. Evidence for increased SARS-CoV-2 susceptibility and COVID-19 severity related to pre-existing immunity to seasonal coronaviruses. *Cell Rep.* **37**, 110169 (2021).
22. Anderson, E. M. et al. Seasonal human coronavirus antibodies are boosted upon SARS-CoV-2 infection but not associated with protection. *Cell* **184**, 1858–1864 e1810 (2021).
23. Begin, P. et al. Convalescent plasma for hospitalized patients with COVID-19: an open-label, randomized controlled trial. *Nat. Med* **27**, 2012–2024 (2021).
24. Herman, J. D. et al. Functional convalescent plasma antibodies and pre-infusion titers shape the early severe COVID-19 immune response. *Nat. Commun.* **12**, 6853 (2021).
25. Bartsch, Y. C. et al. Humoral signatures of protective and pathological SARS-CoV-2 infection in children. *Nat. Med* **27**, 454–462 (2021).
26. Vidarsson, G., Dekkers, G. & Rispen, T. IgG subclasses and allotypes: from structure to effector functions. *Front Immunol.* **5**, 520 (2014).
27. Planas, D. et al. Considerable escape of SARS-CoV-2 Omicron to antibody neutralization. *Nature* **602**, 671–675 (2022).
28. VanBlargan, L. A. et al. An infectious SARS-CoV-2 B.1.1.529 Omicron virus escapes neutralization by therapeutic monoclonal antibodies. *Nat. Med* **28**, 490–495 (2022).
29. Zambrano, L. D. et al. Effectiveness of BNT162b2 (Pfizer-BioNTech) mRNA Vaccination Against Multisystem Inflammatory Syndrome in Children Among Persons Aged 12–18 Years - United States, July–December 2021. *MMWR Morb. Mortal. Wkly Rep.* **71**, 52–58 (2022).
30. Adeniji, O. S. et al. COVID-19 Severity Is Associated with Differential Antibody Fc-Mediated Innate Immune Functions. *mBio* **12**, <https://doi.org/10.1128/mBio.00281-21> (2021).
31. Fuentes-Villalobos, F. et al. Sustained Antibody-Dependent NK Cell Functions in Mild COVID-19 Outpatients During Convalescence. *Front Immunol.* **13**, 796481 (2022).
32. Vicente, M. M. et al. Altered IgG glycosylation at COVID-19 diagnosis predicts disease severity. *Eur J Immunol*, <https://doi.org/10.1002/eji.202149491> (2022).
33. Cheng, H. D. et al. IgG Fc glycosylation as an axis of humoral immunity in childhood. *J. Allergy Clin. Immunol.* **145**, 710–713 e719 (2020).
34. Sagar, M. et al. Recent endemic coronavirus infection is associated with less-severe COVID-19. *J Clin Invest* **131**, <https://doi.org/10.1172/JCI143380> (2021).
35. Grifoni, A. et al. Targets of T Cell Responses to SARS-CoV-2 Coronavirus in Humans with COVID-19 Disease and Unexposed Individuals. *Cell* **181**, 1489–1501 e1415 (2020).
36. Roltgen, K. et al. Immune imprinting, breadth of variant recognition, and germinal center response in human SARS-CoV-2 infection and vaccination. *Cell* **185**, 1025–1040 e1014 (2022).
37. Gagne, M. et al. mRNA-1273 or mRNA-Omicron boost in vaccinated macaques elicits similar B cell expansion, neutralizing responses, and protection from Omicron. *Cell* **185**, 1556–1571 e1518 (2022).
38. Brown, E. P. et al. High-throughput, multiplexed IgG subclassing of antigen-specific antibodies from clinical samples. *J. Immunol. Methods* **386**, 117–123 (2012).
39. Fischinger, S. et al. A high-throughput, bead-based, antigen-specific assay to assess the ability of antibodies to induce complement activation. *J. Immunol. Methods* **473**, 112630 (2019).
40. Karsten, C. B. et al. A versatile high-throughput assay to characterize antibody-mediated neutrophil phagocytosis. *J. Immunol. Methods* **471**, 46–56 (2019).
41. Ackerman, M. E. et al. A robust, high-throughput assay to determine the phagocytic activity of clinical antibody samples. *J. Immunol. Methods* **366**, 8–19 (2011).
42. Garcia-Beltran, W. F. et al. COVID-19-neutralizing antibodies predict disease severity and survival. *Cell* **184**, 476–488 e411 (2021).
43. Thevenot, E. A., Roux, A., Xu, Y., Ezan, E. & Junot, C. Analysis of the Human Adult Urinary Metabolome Variations with Age, Body Mass Index, and Gender by Implementing a Comprehensive Workflow for Univariate and OPLS Statistical Analyses. *J. Proteome Res* **14**, 3322–3335 (2015).
44. Friedman, J. H., Hastie, T. & Tibshirani, R. Regularization Paths for Generalized Linear Models via Coordinate Descent. *J. Stat. Softw.* **33**, 22 (2010).
45. Butts, C. T. network: a Package for Managing Relational Data in R. *J. Stat. Software* **24** (2008).

ACKNOWLEDGEMENTS

We thank Nancy Zimmerman, Mark and Lisa Schwartz, an anonymous donor (financial support), Terry and Susan Ragon, and the SAMANA Kay MGH Research Scholars award for their support. We acknowledge support from the Ragon Institute of MGH, MIT, and Harvard, the Massachusetts Consortium on Pathogen Readiness (MassCPR), the NIH (3R37AI080289-11S1, R01AI146785, U19AI42790-01, U19AI135995-02, U19AI42790-01, 1U01CA260476 – 01, CIVIC75N93019C00052, 5K08HL143183, 1R01HD100022-01 and 3R01HD100022-02S2), the Gates Foundation Global Health Vaccine Accelerator Platform funding (OPP1146996 and INV-001650), and the Musk Foundation.

AUTHOR CONTRIBUTIONS

Y.C.B., J.W.C. and J.K. performed the serological experiments. K.J.D., M.L.S. and A.B.B. performed the neutralization assay. Y.C.B., L.M.Y. and G.A. analyzed and interpreted the data. M.D.B., J.P.D., A.G.E. and L.M.Y. supervised and managed the sample collection. G.A. supervised the project. Y.C.B., L.M.Y. and G.A. drafted the manuscript. All authors critically reviewed the manuscript.

COMPETING INTERESTS

G.A. is a founder of Seromyx Systems, a company developing a platform technology that describes the antibody immune response. G.A.'s interests were reviewed and are managed by Massachusetts General Hospital and Partners HealthCare in accordance with their conflict of interest policies. All other authors have declared that no conflicts of interest exist.

ADDITIONAL INFORMATION

Supplementary information The online version contains supplementary material available at <https://doi.org/10.1038/s41541-022-00575-w>.

Correspondence and requests for materials should be addressed to Lael M. Yonker or Galit Alter.

Reprints and permission information is available at <http://www.nature.com/reprints>

Publisher's note Springer Nature remains neutral with regard to jurisdictional claims in published maps and institutional affiliations.



Open Access This article is licensed under a Creative Commons Attribution 4.0 International License, which permits use, sharing, adaptation, distribution and reproduction in any medium or format, as long as you give appropriate credit to the original author(s) and the source, provide a link to the Creative Commons license, and indicate if changes were made. The images or other third party material in this article are included in the article's Creative Commons license, unless indicated otherwise in a credit line to the material. If material is not included in the article's Creative Commons license and your intended use is not permitted by statutory regulation or exceeds the permitted use, you will need to obtain permission directly from the copyright holder. To view a copy of this license, visit <http://creativecommons.org/licenses/by/4.0/>.

© The Author(s) 2022